

# Molecular Nanoscale Magnetic Refrigerants: A Ferrimagnetic $\{\text{Cu}^{\text{II}}_{15}\text{Gd}^{\text{III}}_7\}$ Cagelike Cluster from the Use of Pyridine-2,6-dimethanol

Despina Dermitzaki,<sup>†</sup> Giulia Lorusso,<sup>‡</sup> Catherine P. Raptopoulou,<sup>§</sup> Vassilis Psycharis,<sup>§</sup> Albert Escuer,<sup>\*,<sup>⊥</sup></sup> Marco Evangelisti,<sup>\*,<sup>‡</sup></sup> Spyros P. Perlepes,<sup>\*,<sup>†</sup></sup> and Theocharis C. Stamatatos<sup>\*,<sup>#</sup></sup>

<sup>†</sup>Department of Chemistry, University of Patras, 265 04 Patras, Greece

<sup>‡</sup>Departamento de Física de la Materia Condensada, Instituto de Ciencia de Materiales de Aragón (ICMA), CSIC-Universidad de Zaragoza, 50009 Zaragoza, Spain

<sup>⊥</sup>Departament de Química Inorgànica, Universitat de Barcelona, Diagonal 645, 08028 Barcelona, Spain

<sup>§</sup>Department of Materials Science, Institute of Advanced Materials, Physicochemical Processes, Nanotechnology and Microsystems, NCSR "Demokritos", 153 10 Agia Paraskevi Attikis, Greece

<sup>#</sup>Department of Chemistry, Brock University, L2S 3A1 St. Catharines, Ontario, Canada

## Supporting Information

**ABSTRACT:** The employment of pyridine-2,6-dimethanol in 3d/4f metal cluster chemistry has afforded a new  $\{\text{Cu}^{\text{II}}_{15}\text{Gd}^{\text{III}}_7\}$  cagelike molecule with a beautiful structure built by fused triangular subunits; the compound exhibits an overall ferrimagnetic behavior with an appreciable ground-state spin value and shows promise as a low-temperature magnetic refrigerant.

One of the most fascinating challenges in modern coordination chemistry is undoubtedly the combination of an aesthetically pleasing structure with an interesting physical property or occasionally with more than one property within the same molecular species. Polynuclear heterometallic 3d/4f metal compounds are clearly excellent candidates to satisfy such expectations.<sup>1</sup> This is due to the pronounced ability of these metal ions to form and stabilize high-nuclearity and structurally complicated metal–oxido/hydroxido inorganic cores surrounded in the periphery by organic bridging/chelating ligands. The type and nature of the latter groups play a significant role in the self-assembly synthesis of new polynuclear compounds, and the choice of a small, flexible, and polydentate ligand (or ligand “blend”) seems to be an attractive route. Polynuclear 3d/4f metal complexes (or coordination clusters) have shown a remarkable ability to act either as single-molecule magnets<sup>2</sup> mainly when the f-block ions are highly anisotropic and possess a significant spin (i.e., Dy<sup>III</sup>, Tb<sup>III</sup>) or as magnetic refrigerants<sup>3</sup> when the molecules are isotropic and high-spin, conditions which are fulfilled by the copresence of, for instance, Gd<sup>III</sup> and Cu<sup>II</sup> metal ions.

Magnetic refrigeration is based on the magnetocaloric effect (MCE). MCE deals with a change of the magnetic entropy upon application of a magnetic field and can be used for cooling purposes via adiabatic demagnetization.<sup>4</sup> In the last 6 years, the systematic exploration of the MCE in isotropic molecular magnetic compounds has demonstrated enormous values, larger than those observed on lanthanide alloys and magnetic nanoparticles.<sup>3,4</sup>

The MCE is greatly enhanced in molecules containing isotropic magnetic ions with large total spin  $S$ .<sup>3</sup> Taking this

into account, Cu<sup>2+</sup>/Gd<sup>3+</sup> complexes seem to be very good candidates for molecular refrigerants because the Gd<sup>3+</sup> ion has an isotropic  $f^7$  configuration and the Cu<sup>2+</sup>/Gd<sup>3+</sup> magnetic interactions are generally ferromagnetic in nature, leading to ground states with increased and large-spin multiplicity.<sup>5</sup> Further, the Cu<sup>2+</sup>/Gd<sup>3+</sup> magnetic exchange interactions are very weak because of the very efficient shielding of the Gd<sup>3+</sup> 4f orbitals by the fully occupied 5s and 5p orbitals,<sup>5</sup> and this generates multiple low-lying excited and field-accessible states, each of which can contribute to the magnetic entropy of the system. The magnetic entropy is related to the spin by  $S_m = R \ln(2S + 1)$ , where  $R$  is the gas constant. To date, clusters with very large MCE include homometallic  $\{\text{Gd}_2\}$ <sup>6a</sup> and  $\{\text{Gd}_{24}\}$ <sup>1b</sup> and heterometallic  $\{\text{Ni}_{12}\text{Gd}_{36}\}$ <sup>6b</sup> and  $\{\text{Mo}_4\text{Gd}_{12}\}$ <sup>6c</sup> complexes with  $-\Delta S_m$  values of  $\sim 40$ , 46.1, 36.3, and 35.3 J kg<sup>-1</sup> K<sup>-1</sup>, respectively, for liquid-helium temperatures and  $\Delta B_0 = 7$  T.

In simple words, to construct polynuclear metal complexes behaving as magnetic coolers, we need a metal–ligand “blend”, which will guarantee aggregation of the metal ions into a large-nuclearity motif and will produce a ferro- or ferrimagnetic system with negligible anisotropy. Toward this end, we have decided to employ the tridentate (N, O, O) ligand pyridine-2,6-dimethanol (pdmH<sub>2</sub>) in heterometallic copper(2+)/gadolinium(3+) carboxylate chemistry as a means of satisfying the above requirements. Thus, the reaction of Cu(O<sub>2</sub>CPh)<sub>2</sub>·2H<sub>2</sub>O, Gd(NO<sub>3</sub>)<sub>3</sub>·6H<sub>2</sub>O, pdmH<sub>2</sub>, and NEt<sub>3</sub> in a 1:1:1:1 molar ratio in MeCN led to a blue suspension, which upon filtration gave a pale-blue filtrate. The latter was allowed to slowly evaporate at room temperature, yielding after 10 days blue crystals of  $[\text{Cu}_{15}\text{Gd}_7(\text{OH})_6(\text{CO}_3)_4(\text{O}_2\text{CPh})_{19}(\text{pdm})_9(\text{pdmH}_2)_3(\text{H}_2\text{O})_2]$  (**1**) in 20% yield.<sup>7</sup> The formula of **1** is based on metric parameters, charge-balance considerations, and bond-valence-sum calculations on the O atoms. The CO<sub>3</sub><sup>2-</sup> ions are presumably derived from the fixation of atmospheric CO<sub>2</sub>.<sup>8</sup> Identification of the CO<sub>3</sub><sup>2-</sup> ions (vs NO<sub>3</sub><sup>-</sup>) in **1** was determined via careful consideration of the X-ray diffraction data and observation of carbonate-related IR absorption bands at  $\sim 1400$  and 845 cm<sup>-1</sup>.<sup>8</sup> Although rare, the

Received: August 3, 2013

Published: September 5, 2013

copresence of fully deprotonated and neutral forms of an alkoxide-based ligand, as the  $\text{pdm}^{2-}/\text{pdmH}_2$  combination in **1**, is with precedence in 3d/4f metal cluster chemistry.<sup>9</sup>

The structure of **1** consists of a  $\{\text{Cu}^{\text{II}}_{15}\text{Gd}^{\text{III}}_7\}$  cage-like cluster (Figure 1, left) with  $C_3$  crystallographic symmetry (the 3-fold axis

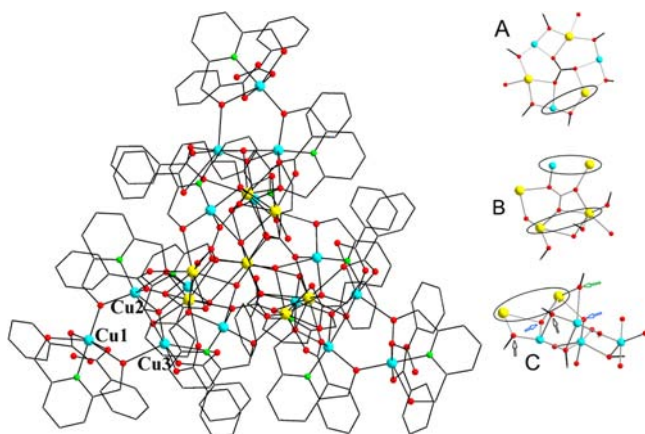


**Figure 1.** Structure of **1** (left) and the three different types of constituent subunits of its core (right). H atoms are omitted for clarity. The circles and arrows indicate the connection “points” between the subunits. Color scheme:  $\text{Cu}^{\text{II}}$ , cyan;  $\text{Gd}^{\text{III}}$ , yellow; O, red; N, green; C, gray.

passing from the central, unique Gd2 atom) and irregular topology resulting from many fused triangular subunits. The metal ions within the core of **1** (Figure S1 in the Supporting Information, SI) are bridged by six  $\mu_3\text{-OH}^-$  ions, three  $\eta^2:\eta^2:\eta^2:\mu_5$  and an  $\eta^2:\eta^2:\eta^2:\mu_6$   $\text{CO}_3^{2-}$  ions, and the alkoxido arms of nine  $\eta^2:\eta^1:\eta^3:\mu_4$   $\text{pdm}^{2-}$  and three  $\eta^1:\eta^1:\eta^2:\mu$   $\text{pdmH}_2$  groups (Figure S2 in the SI). Peripheral ligation about the core is provided by the chelating part of the  $\text{pdm}^{2-}/\text{pdmH}_2$  groups, two terminal  $\text{H}_2\text{O}$  molecules, and 19  $\text{PhCO}_2^-$  ligands. The latter are arranged into four classes: seven are monodentate, with the dangling O atoms hydrogen-bonded to the OH groups of the  $\text{pdmH}_2$  ligands, six are bidentate-chelating, three are  $\eta^1:\eta^1:\mu$ , and three  $\eta^1:\eta^2:\mu_3$ . All Cu ions are six-coordinate with distorted octahedral geometries except Cu4 and Cu5 (and their symmetry-related partners), which are five-coordinate with almost perfect square-pyramidal geometries ( $\tau = 0.03$  and  $0.06$ , respectively). The Gd ions are nine-coordinate (Gd1 and Gd2) and eight-coordinate (Gd3) with very distorted geometries. The complicated core of **1** can be conveniently described as consisting of a central, nonplanar,  $\mu_6$ -carbonato-bridged  $\{\text{Cu}_3\text{Gd}_3\}$  unit (A), each  $\text{Cu}\cdots\text{Gd}$  edge of which is additionally linked to three  $\text{Gd}^{3+}$  ions by a  $\mu_3\text{-CO}_3^{2-}$  (B). The resulting inner  $\{\text{Cu}_3\text{Gd}_7(\text{CO}_3)_4\}^{19+}$  subcore (A + B, Figure 1, right) is further bridged to three extrinsic  $\{\text{Cu}_4\}$  subunits (C, Figure 1, right) through the  $\mu_3$ -hydroxido and alkoxido groups. Finally, regarding the topology of the seven  $\text{Gd}^{\text{III}}$  atoms, this could be roughly described as distorted, capped trigonal antiprismatic, with Gd2 occupying the capping site (Figure S3 in the SI). The space-filling representation of **1** reveals its large nanometer-sized structure with an average diameter of  $\sim 2.6$  nm, as defined by the longest  $\text{H}\cdots\text{H}$  distance (Figure S4 in the SI). Complex **1** is the fourth largest Cu/Gd cluster isolated to date after the  $\{\text{Cu}_{24}\text{Gd}_8\}$ ,<sup>10a</sup>  $\{\text{Cu}_{24}\text{Gd}_6\}$ <sup>10b</sup> and  $\{\text{Cu}_{36}\text{Gd}_{24}\}$ <sup>10c</sup> cages, while it is one of the highest-nuclearity heterometallic compounds<sup>10c</sup> showing MCE (vide infra).

Solid-state direct-current magnetic susceptibility ( $\chi_M$ ) data on dried  $1\cdot 2\text{H}_2\text{O}$  were collected in the 2.0–300 K range in applied

fields of 0.3 T (300–30 K) and 0.02 T (30–2 K) to avoid saturation effects and are plotted as  $\chi_M T$  vs  $T$  in Figure 2. The

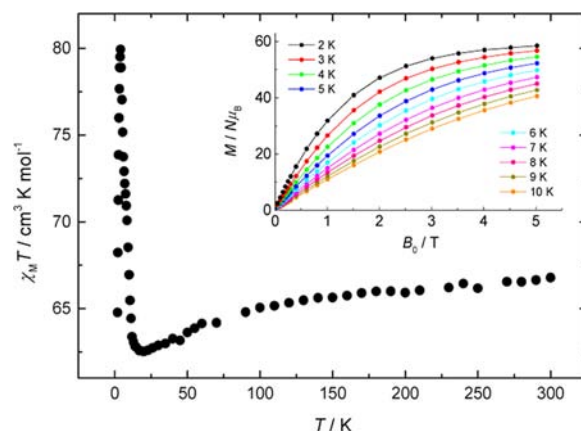


**Figure 2.**  $\chi_M T$  vs  $T$  plot of **1**. Inset: Field-dependent magnetization plot at the indicated temperatures. Lines are guides to the eye.

$\chi_M T$  at 300 K is  $66.79 \text{ cm}^3 \text{ K mol}^{-1}$ , essentially equal to the calculated value of  $66.98 \text{ cm}^3 \text{ K mol}^{-1}$  for 15  $\text{Cu}^{\text{II}}$  ( $S = 1/2$ ) and 7  $\text{Gd}^{\text{III}}$  ( $S = 7/2, L = 0$ ) noninteracting ions, assuming an average  $g$  value of 2.10. It slowly decreases with decreasing temperature to a value of  $62.53 \text{ cm}^3 \text{ K mol}^{-1}$  at 20 K and then rapidly increases to  $79.93 \text{ cm}^3 \text{ K mol}^{-1}$  at 4.0 K before it drops to  $64.78 \text{ cm}^3 \text{ K mol}^{-1}$  at 2.0 K. The shape of the  $\chi_M T$  vs  $T$  plot indicates that both antiferro- and ferromagnetic exchange interactions dominate at different  $T$  regions. It is well established that alkoxido-bridged  $\text{Cu}^{2+}$  ions, with  $\text{Cu}-\text{OR}-\text{Cu}$  bond angles larger than  $95^\circ$ , are antiferromagnetically coupled, and thus the former types of interactions in **1** can be reasonably assigned to  $\text{Cu}^{2+}\cdots\text{Cu}^{2+}$  and the latter to  $\text{Cu}^{2+}\cdots\text{Gd}^{3+}$  or  $\text{Gd}^{3+}\cdots\text{Gd}^{3+}$ . The ground-state spin value of this ferrimagnetic system cannot be accurately determined because of its complicated structure with many fused triangular subunits. The magnetization measurements (inset of Figure 2) show a trend for saturation at a value of  $58.3 N\mu_B$  at the highest fields and lowest temperatures employed, suggesting a net spin state of  $S = 58/2 = 29$ . This can be tentatively rationalized assuming all of the  $\text{Cu}^{\text{II}}\cdots\text{Gd}^{\text{III}}$  interactions to be ferromagnetic ( $12 \times 1/2 + 7 \times 7/2 = 61/2$ ) and the interactions between the three extrinsic  $\text{Cu}^{\text{II}}$  ions ( $\text{Cu1}$ ,  $\text{Cu1a}$ , and  $\text{Cu1b}$ ) with their directly bridged  $\text{Cu}^{\text{II}}$  ions ( $\text{Cu2/Cu3}$ ,  $\text{Cu2a/Cu3a}$ , and  $\text{Cu2b/Cu3b}$ ) to be antiferromagnetic, thus forcing those three  $S = 1/2$  spins to align antiparallel to all other and resulting in a field-stabilized spin state of  $S = 61/2 - 3/2 = 58/2$ . This is likely to occur because the average  $\text{Cu1}-\text{O}-\text{Cu2/3}$  bond angle is  $\sim 120^\circ$ , which will be antiferromagnetic and stronger than the  $\text{Cu2}-\text{O}-\text{Cu}_3$  interaction (average angle of  $\sim 101^\circ$ ).<sup>11a</sup>

The large value for the magnetization makes **1** a possible candidate for low-temperature magnetic cooling, and we have thus evaluated its MCE, which includes calculation of the magnetic entropy change  $\Delta S_m$  and adiabatic temperature change  $\Delta T_{\text{ad}}$  for selected applied field changes  $\Delta B_0$ , from the measured heat capacity (Figure S5 in the SI) and magnetization (Figure 2). As for the former,  $\Delta S_m$  can be obtained from the  $T$  and field dependencies of the entropy. The results are shown in Figure 3. We report an appreciable value of  $-\Delta S_m$ , which reaches  $\sim 22.2 \text{ J kg}^{-1} \text{ K}^{-1}$  at  $T = 2.5 \text{ K}$  for  $\Delta B_0 = 7 \text{ T}$ . This is what we could expect considering the large net magnetic moment and negligible anisotropy of the molecule, as well as the weak intracluster interactions involving  $\text{Gd}^{\text{III}}$  ions that lead to low-lying excited

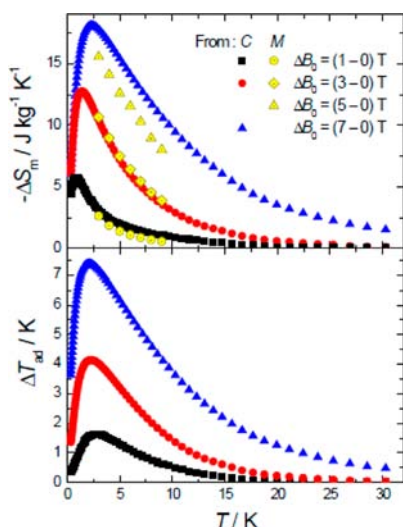


**Figure 3.** (top)  $T$  dependencies of the magnetic entropy change as obtained from the heat capacity ( $C$ ) and magnetization ( $M$ ) data, for the indicated applied field changes. (bottom)  $T$  dependencies of the adiabatic temperature change obtained from  $C$  data, for the indicated applied field changes.

spin states.<sup>3</sup> However, this value is still lower than the maximum entropy value per mole ( $25R \sim 33.5 \text{ J kg}^{-1} \text{ K}^{-1}$ ) for  $15 \text{ Cu}^{\text{II}}$  and  $7 \text{ Gd}^{\text{III}}$  fully decoupled ions. In the  $2 \text{ K} < T < 6 \text{ K}$  range, the zero-field magnetic entropy shows a “plateau” at a considerably lower value, i.e.,  $\sim 17R$ , indeed (Figure S5 in the SI). This is ascribed to the overall ferrimagnetism of **1**, which results from the relatively strong antiferromagnetic  $\text{Cu}^{\text{II}} \cdots \text{Cu}^{\text{II}}$  exchange, and it is thus clear that this type of interaction is the least favorable for observing the maximum MCE.<sup>11b</sup> Fields higher than  $7 \text{ T}$  are needed in order to fully break the antiferromagnetic exchanges (Figure S5 in the SI). With regards to the adiabatic temperature change, Figure 3 (bottom) shows that  $\Delta B_0 = 7 \text{ T}$  provides a maximum  $\Delta T_{\text{ad}} = 7.5 \text{ K}$  for the same temperatures at which we observe the  $-\Delta S_{\text{m}}$  maxima. When  $\Delta B_0$  was lowered to  $3$  and  $1 \text{ T}$ ,  $\Delta T_{\text{ad}}$  decreases to  $4.2$  and  $1.7 \text{ K}$ , respectively. Therefore, the field dependence of  $\Delta T_{\text{ad}}$  increases slightly from nearly  $\sim 1$  to  $\sim 1.7 \text{ K T}^{-1}$ , respectively, setting this material as a promising refrigerant for this low-temperature region.<sup>3,4,12</sup> The  $-\Delta S_{\text{m}}$  value of  $\sim 22.2 \text{ J kg}^{-1} \text{ K}^{-1}$  for **1** is the second largest in  $\text{Cu}/\text{Gd}$  cluster chemistry, after the value of  $\sim 31 \text{ J kg}^{-1} \text{ K}^{-1}$  reported for a  $\{\text{Cu}_5\text{Gd}_4\}$  compound.<sup>11a</sup>

In conclusion, we have shown that the  $\text{Cu}^{2+}/\text{Gd}^{3+}/\text{PhCO}_2^-/\text{pdmH}_2$  system is a promising reaction scheme to follow, not only for the synthesis of new high-nuclearity heterometallic complexes with beautiful topologies but also for magnetically interesting species with promising low- $T$  MCE. We are currently focusing on the effect of the nature of the carboxylate group on the  $\{\text{Cu}_{15}\text{Gd}_7\}$  identity and the isolation of  $\text{Cu}^{2+}/\text{Gd}^{3+}$  magnetic coolers with larger MCE.

## ■ ASSOCIATED CONTENT

### 📄 Supporting Information

Crystallographic data (CIF format), synthetic details, and various figures for **1**. This material is available free of charge via the Internet at <http://pubs.acs.org>.

## ■ AUTHOR INFORMATION

### Corresponding Authors

\*E-mail: [albert.escuer@ub.edu](mailto:albert.escuer@ub.edu).

\*E-mail: [evange@unizar.es](mailto:evange@unizar.es).

\*E-mail: [perlepes@upatras.gr](mailto:perlepes@upatras.gr).

\*E-mail: [tstamatatos@brocku.ca](mailto:tstamatatos@brocku.ca).

## Notes

The authors declare no competing financial interest.

## ■ ACKNOWLEDGMENTS

This work was supported by the CICYT (Project CTQ2012-30662) and Excellence in Research ICREA-Academia Award (to A.E.), the MINECO (Grant MAT2012-38318-C03 to M.E. and G.L.), an EU Marie Curie IEF (Grant PIEF-GA-2011-299356 to G.L.), the ARISTEIA Action (Project code 84, acronym MAGCLOPT) of the Operational Programme “Education and Lifelong Learning”, cofunded by ESF and National Resources (to S.P.P.), and the NSERC Discovery Grant (to T.C.S.).

## ■ REFERENCES

- (1) (a) Zheng, Y.-Z.; Evangelisti, M.; Tuna, F.; Winpenny, R. E. P. *J. Am. Chem. Soc.* **2012**, *134*, 1057. (b) Chang, L.-X.; Xiong, G.; Wang, L.; Cheng, P.; Zhao, B. *Chem. Commun.* **2013**, *49*, 1055.
- (2) Holyńska, M.; Premužić, Jeon, I.-R.; Wernsdorfer, W.; Clérac, R.; Dehnen, S. *Chem.—Eur. J.* **2011**, *17*, 9605.
- (3) Evangelisti, M.; Brechin, E. K. *Dalton Trans.* **2010**, *39*, 4672.
- (4) Evangelisti, M.; Luis, F.; de Jongh, L. J.; Affronte, M. *J. Mater. Chem.* **2006**, *16*, 2534.
- (5) Andruh, M.; Costes, J. P.; Diaz, C.; Gao, S. *Inorg. Chem.* **2009**, *48*, 3342.
- (6) (a) Evangelisti, M.; Roubeau, O.; Palacios, E.; Camón, A.; Hooper, T. N.; Brechin, E. K.; Alonso, J. *Angew. Chem., Int. Ed.* **2011**, *50*, 6606. (b) Peng, J.-B.; Zhang, Q.-C.; Kong, X.-J.; Ren, Y.-P.; Long, L.-S.; Huang, R.-B.; Zheng, L.-S.; Zheng, Z. *Angew. Chem., Int. Ed.* **2011**, *50*, 10649. (c) Zheng, Y.; Zhang, Q.-C.; Long, L.-S.; Huang, R.-B.; Müller, A.; Schnack, J.; Zheng, L.-S.; Zheng, Z. *Chem. Commun.* **2013**, *49*, 36.
- (7) Anal. Calcd (found) for  $1 \cdot 2\text{H}_2\text{O}$ : C, 41.34 (41.16); H, 3.12 (3.02); N, 2.62 (2.86). Crystal structure data for  $1 \cdot 4.5\text{MeCN} \cdot 1.5\text{H}_2\text{O}$ :  $\text{C}_{230}\text{H}_{211.5}\text{Cu}_{15}\text{Gd}_7\text{N}_{16.5}\text{O}_{83.5}$ ,  $M_w = 6596.51$ , hexagonal, space group  $R\bar{3}$  with  $a = b = 34.3349(6) \text{ \AA}$ ,  $c = 37.9490(7) \text{ \AA}$ ,  $V = 38743.8(12) \text{ \AA}^3$ ,  $T = 160(2) \text{ K}$ ,  $Z = 6$ ,  $R1 [I > 2\sigma(I)] = 0.0506$ ,  $wR2 = 0.1236$  ( $F^2$ , all data).
- (8) (a) Langley, S. K.; Moubaraki, B.; Murray, K. S. *Inorg. Chem.* **2012**, *51*, 3947 and references cited therein. (b) Tian, H.; Zhao, L.; Guo, Y.-N.; Guo, Y.; Tang, J.; Liu, Z. *Chem. Commun.* **2012**, *48*, 708.
- (9) Mereacre, V.; Ako, A. M.; Clérac, R.; Wernsdorfer, W.; Hewitt, I. J.; Anson, C. E.; Powell, A. K. *Chem.—Eur. J.* **2008**, *14*, 3577.
- (10) (a) Baskar, V.; Gopal, K.; Helliwell, M.; Tuna, F.; Wernsdorfer, W.; Winpenny, R. E. P. *Dalton Trans.* **2010**, *39*, 4747. (b) Zhang, J.-J.; Hu, S.-M.; Xiang, S.-C.; Sheng, T.; Wu, X.-T.; Li, Y.-M. *Inorg. Chem.* **2006**, *45*, 7173. (c) Leng, J.-D.; Liu, J.-L.; Tong, M.-L. *Chem. Commun.* **2012**, *48*, 5286.
- (11) (a) Langley, S.; Chilton, N. F.; Moubaraki, B.; Hooper, T.; Brechin, E. K.; Evangelisti, M.; Murray, K. S. *Chem. Sci.* **2011**, *2*, 1166. (b) Hooper, T. N.; Schnack, J.; Piligkos, S.; Evangelisti, M.; Brechin, E. K. *Angew. Chem., Int. Ed.* **2012**, *51*, 4633.
- (12) Colacio, E.; Ruiz, J.; Lorusso, G.; Brechin, E. K.; Evangelisti, M. *Chem. Commun.* **2013**, *49*, 3845.